Water Air Soil Pollut (2015) 226: 70
DOI 10.1007/s11270-015-2301-1

How the Dyes Are Degraded/Mineralized in a Photocatalytic System? The Possible Role of Auxochromes

M. Aslam · Iqbal M. I. Ismail · S. Chandrasekaran · Huda A. Qari · A. Hameed

Received: 3 September 2014 / Accepted: 12 January 2015 / Published online: 25 February 2015

Abstract The capability of W^{6+}-impregnated ZnO photocatalysts for sunlight mineralization of a variety of structurally different dyes has been investigated. Compared to bare ZnO, the W^{6+}-loaded photocatalysts showed significantly higher activity for the decolorization as well as mineralization of dyes, and complete mineralization was noticed in a short span of 150 min. The results obtained by various analytical tools were correlated to estimate the mechanistic aspects of the decolorization/mineralization process and to identify the nature of the oxidizing species involved in the process. A strong dependence of the decolorization/mineralization process was observed on the nature and number of auxochromes attached to color-generating conjugated system. The rapid decolorization/mineralization of the dyes and release of corresponding anions with the decolorization of dyes suggested the involvement of charged rather than radical reactive oxygen species (ROS) in the oxidation process. Langmuir-Hinshelwood kinetic model was found to be best suited for evaluating the kinetics of mineralization process. The effectiveness of the catalysts for the decolorization/mineralization of a mixture of dyes was also examined. The suitability of the catalysts for successive use in sunlight exposure was also evaluated.

Keywords Decolorization · Photocatalysis · Sunlight · Dyes · Auxochromes

1 Introduction

Water is the lifeline of living beings on earth. The presence of color of unspecified origin raises objections on water quality for living, especially human beings consumption (ETAD 1997). Colorants or dyes are characterized by large molecular structures composed of fused aromatic and nonaromatic rings with established conjugation and auxochromes that engender color (Singh and Arora 2011; Christie 2001). Among the chemical processing industries, the textile sector is the major producer of highly colored wastewater due to the ample use of colorants (dyes) in the fabric dying process (Makita and Harata 2008). Other industries that add color discharge include dyestuff manufacturing industries, distilleries, and tanneries (Martinez and Brillas 2009; Boyter 2007). It has been estimated that

M. Aslam · I. M. I. Ismail · S. Chandrasekaran · A. Hameed (✉)
Centre of Excellence in Environmental Studies (CEES), King Abdulaziz University, Jeddah 21589, Saudi Arabia
e-mail: afmuhammad@kau.edu.sa

I. M. I. Ismail
Chemistry Department, Faculty of Science, King Abdulaziz University, Jeddah 21589, Saudi Arabia

H. A. Qari
Biological Department, Faculty of Science, King Abdulaziz University, Jeddah 21589, Saudi Arabia

A. Hameed
National Centre for Physics, Quaid-e-Azam University, Islamabad 44000, Pakistan

approximately 15 % of the total dye stuff used in the textile sector for various processes is discharged as an industrial effluent without any treatment (Cho and Zoh 2007) that leads to adverse environmental and health effects; therefore, complete removal of dyes from the industrial wastewater is essential before being discharged to water channels. The situation is further aggravated when the dyes present in wastewater undergo oxidation and reduction, due to a variety of environmental factors such as pH, light, temperature, and microorganisms, generating a secondary stream of potentially carcinogenic or mutagenic compounds that can be lethal towards living organisms including humans in the ecosystem (Khataee et al. 2009). Therefore, the complete removal of these toxic dyes, without leaving any toxic by-product or intermediates, is highly desirable.

Among the traditional physiochemical methods for the removal of dyes, adsorption is regarded as a viable option; however, the capacity and the safe disposal of dye-loaded adsorbents are a restraining factor in its widespread applicability (Chong et al. 2010). The requirements of selective microorganisms, prolonged incubation periods, and controlled temperature conditions limit the use of biological means for dye removal. Oxidation technologies that lead to either complete mineralization or transformation to less toxic oxygenate have gathered considerable attention for the elimination of dyes in the recent years (Chong et al. 2010; Ligrini et al. 1993; Rauf and Ashraf 2009). Photocatalysis, being the part of oxidation technologies, is considered as s solution provider for the cost-effective removal of dyes from an industrial effluent (Hernández-Alonso et al. 2009; Fujishima et al. 2000; Jiuhui 2008; Bhatkhande et al. 2002; Lettmann et al. 2001; Lazar et al. 2012; Mills et al. 1993) where the conversion of light energy into chemical energy by the semiconductor nontoxic materials, with the in situ generation of oxidizing species, leads to the complete mineralization of dyes (Sotto et al. 2010; Ahmed et al. 2010). Since carried out at ambient conditions, photocatalytic processes do not require extreme operational conditions of pressure and temperature or addition of expensive oxidizing agents for the generation of oxidizing species (Chatterjee and Dasgupta 2005; Lam et al. 2012; Hameed et al. 2011; Neppolian et al. 2003).

Currently, in photocatalysis, a variety of artificial light sources are in use for the initiation of the excitation process at the surface of the semiconductor and the generation of oxidizing species which are suitable for the study of process at the lab scale but loosen economic and operational viability in large-scale use (Fang et al. 2007). The wide-ranging commercial applicability of photocatalysis requires the utilization of a cheaply available, high-intensity, polychromatic, and self-sustained excitation source. Sunlight being comprised of about ~42 % visible and ~5 % UV light (Fang et al. 2007) is an appropriate alternative to the artificial energy sources for use in photocatalytic processes. However, the nonavailability of sunlight/visible light-responsive photocatalysts limits the use of this renewable and intense excitation source for photocatalytic environmental applications. Hence, it is highly desirable either to explore the new sunlight active photocatalysts or to enhance the capability of the existing photocatalysts such as TiO_2 and ZnO by applying suitable surface or structural modifications to harvest the major portion of sunlight with sufficiently high activity. Although TiO_2 is the most studied active photocatalysts (Chong et al. 2010); nevertheless, ZnO, due to its higher absorption cross section and comparable activity, is a better choice than TiO_2 for use in sunlight photocatalytic decontamination processes (Sakthivel et al. 2003). The photocatalytic properties of ZnO are strongly dependent on its structure, including the morphology, aspect ratio, size, orientation, and crystal structure. ZnO, with a band gap of 3.2 eV, is a highly fluorescent material that reflects the high recombination rate of charge carriers. Secondly, its surface undergoes anodic corrosion under illumination (Velmurugan and Swaminathan 2011). It has been proposed that the drawbacks associated with ZnO can be eliminated, and its activity can be enhanced in the solar spectrum (Hameed et al. 2008, 2009a, b, c). Several approaches are proposed in the literature (Rehman et al. 2009; Zhang 1997; Rolison 2003; Bell 2003) to make ZnO responsive in the sunlight exposure. Among the proposed strategies, the alteration of ZnO surface by metal ion (impregnation) or altering its band structure by metal ion insertion (doping) is being considered widely. Photocatalysis being a surface phenomenon (Fujishima et al. 2008), the surface modification through metal ion impregnation, can lead to better results rather than altering the crystal structure by metal ion insertion. Metal ion impregnation not only maximizes its photocatalytic efficiency but also shifts the photoresponse of ZnO in the visible region (Sun et al. 2011).

The photocatalytic decolorization of dyes has been reviewed in detail (Ahmed et al. 2010) where the majority of the studies is carried out using TiO_2 and artificial light sources. Secondly, most of the studies lack the explanation of the mechanistic aspects of dye

decolorization in aqueous photocatalytic system. Very few are available in the literature regarding the evaluation of the photocatalytic activity of ZnO either bare or modified (doped/impregnated), in natural sunlight. In the area of photocatalyst development, dyes are often used as substrates to evaluate the photocatalytic activity of synthesized or modified catalysts. However, the studies covering the modes of degradation/decolorization/ mineralization of dyes and the identification of the oxidizing species involved in the process are very rare. Usually, decolorization of the dye substrate is wrongly quoted as degradation. In our opinion, the decolorization supported by mineralization (total organic carbon (TOC) removal) actually determines the degradation of dye. The degradation without the change in TOC should be treated as decolorization.

The present study is focused upon sunlight-assisted photocatalysis of six model dyes using W^{6+}-impregnated ZnO. The selection of dyes rhodamine B (RhB), alizarin yellow R (AY), methyl orange (MO), congo red (CR), indigo carmine (IC), and rose bengal (RB) is based on their chemical structure, absorption spectra, and the auxochromes attached to the conjugated system with the aim to explore the plausible route for the decolorization as well as mineralization. High-performance liquid chromatography (HPLC) was used to verify the formation of intermediates. The decolorization of the dyes was monitored by UV-visible spectroscopy, while the mineralization of the carbon contents of the particular dye was estimated by measuring the TOC. The concentration of released ions, estimated by ion chromatography, in the solution was used as a marker for the identification of oxidizing agents involved in the decolorization and mineralization process and their probable interaction sites in the dye molecules. In addition, the suitable kinetic model was used to evaluate the kinetics of decolorization and mineralization process. The efficacy of the catalyst was established for the decolorization/mineralization of mixture of abovementioned dyes containing 10 ppm of each dye maintaining 60 ppm of overall dye concentration in the solution.

2 Experimental Details

The impregnation of ZnO with W^{6+} ions was achieved by wet impregnation. The detailed procedure for the synthesis and characterization of the impregnated catalysts is detailed in our previous communication (Hameed et al. 2014).

Prior to sunlight exposure, 150 cm^3 of catalyst-dye suspension containing 30 ppm dye solution and 100 mg photocatalyst was kept in the dark for 1 h to attain adsorption equilibrium. For photocatalytic experiments, the catalyst-dye suspension was exposed to sunlight ($900–1100\times10^2$ lx) in a glass reactor (120×30 mm). It was noticed that the intensity of sunlight affects the progress of photocatalytic experiments, while no significant effect due to the change in the angle of incidence was observed. The intensity of sunlight was monitored at regular intervals during the course of studies for optimum comparison. The progress of the dye decolorization process was monitored by analyzing the samples at regular intervals using a UV-visible spectrometer (Shimadzu UV-1800) after completely removing the catalyst. The mineralization of the respective dye was evaluated by TOC measurements using TOC-V_{CPH} total carbon analyzer supplied by Shimadzu Corporation, Japan. Dionex ion chromatograph (ICS-5000 + EG Eluent Generator; Thermo Scientific, USA) was used to estimate the inorganic ions released during the decolorization/mineralization process. The samples collected after 20 min of sunlight exposure were analyzed by HPLC (SPD-20A; Shimadzu, Japan) to estimate the formation of intermediates. The reproducibility of results and the calibration of all the equipment were ensured on a regular basis.

3 Results and Discussion

3.1 Characterization

The characterization of the W^{6+}-impregnated catalysts by UV-visible diffuse reflectance spectroscopy (DRS), photoluminescence (PL) spectroscopy, X-ray photoelectron spectroscopy (XPS), X-ray diffraction analysis (XRD), and field emission scanning electron microscopy (FESEM) is discussed in detail in our earlier communication (Hameed et al. 2014).

3.2 Photocatalytic Degradation of Dyes

The generation and population of reactive oxygen species (ROS) in an aqueous photocatalytic system is primarily dependent on the ability of the photocatalyst to generate charge carriers (e^-, h^+) with the absorption of photons and, finally, its capability to deliver these to the adsorbed species like water and oxygen before being

squandered in the recombination process. The presence of charge-trapping entities, for enhancing the lifetime of excited states and productive use of photogenerated redox couple, is mandatory to avoid nonproductive loss. The favorable valance band edge ($E_{vb} \geq 1.23$ V) and conduction band edge ($E_{cb} \leq -0.28$ V) facilitates the generation of hydroxyl radicals (Eq. 1) and superoxide anion radicals ($O_2^{\cdot -}$). The source of oxygen (O_2) for superoxide anion radical ($O_2^{\cdot -}$) formation (Eq. 2) is either the dissolved/adsorbed oxygen already present in the system or produced in situ as a result of water oxidation by photogenerated holes (Eq. 3).

$$h^+ + H_2O \rightarrow H^+ + HO^{\cdot} \quad (1)$$

$$O_2(\text{dissolved/adsorbed}) + e^-_{CB} \rightarrow O_2^{\cdot -} \quad (2)$$

$$HO^{\cdot} + HO^{\cdot} \rightarrow H_2O + \S O_2 \quad (3)$$

The characteristic features of dyes are the presence of chromophores, conjugated system composed of alternating double and single bond, fused rings, stabilizing effect of resonance, and auxochromes (Abrahart 1977). All these features collectively impart color to the dyes that exhibit strong absorption in the visible region of spectrum, i.e., 420–800 nm. The position of the absorption maximum is systematized by the auxochromes attached to the conjugated system. The loss of any of the abovementioned features results in decolorization of dye. Being composed of large resonance/conjugation-stabilized molecules, along with the potential environmental concerns associated, dyes are widely used as substrates for the evaluation of the photocatalytic activity. Any alteration in the dye structure because of the interaction of oxidizing species produced in the aqueous phase photocatalytic system may end up in the decolorization of the dye. The loss of color does not essentially mean the complete removal of dye along with the removal of all the intermediate decolorization products. In a photocatalytic system, mainly the decolorization of dye is accomplished by either direct or indirect photocatalysis. The decolorization of dyes via direct photocatalysis mode is achieved by the sole interaction of reactive oxygen species with the dye substrate. The indirect photocatalysis mode operates for those dyes that show strong absorption in the excitation region of the photocatalyst, and dye molecules facilitate their own decolorization by injecting the energy in the photocatalyst for the generation of oxidizing species after being excited by photon absorption. The degradation of organic substrates through the oxidation by the photogenerated holes is also probable. In our opinion, this mode may be applicable to lighter molecules with sufficient donate-able electrons, which the dyes lack due to conjugation, delocalization, and resonance. The bulky structure of dyes is an additional restraint in the applicability of this mode. Additionally, in the presence of highly oxidizing species like superoxide anion radicals ($O_2^{\cdot -}$), it may be hard to estimate the additional contribution of hole oxidation mode. For dyes, h^+ oxidation may lead to decolorization (due to the loss of conjugation); however, the complete degradation is doubtful. The three possible modes of the dye degradation are presented below.

- Direct photocatalysis

$$O_2^{\cdot -} + \text{Dye} \rightarrow \text{Intermediates} \quad (4)$$

$$HO^{\cdot} + \text{Dye} \rightarrow \text{Intermediates} \quad (5)$$

$$O_2^{\cdot -},\ HO^{\cdot} + \text{Intermediates} \rightarrow CO_2 + H_2O \quad (6)$$

- Dye-assisted indirect/charge transfer photocatalysis

$$\text{Dye} + h\nu \rightarrow \text{Dye}^* \quad (7)$$

$$\text{Dye}^* + \text{PC} \rightarrow \text{PC}\left(e^-_{CB} + h^+_{VB}\right) + \text{Dye} \quad (\text{PC} = \text{photocatalyst}) \quad (8)$$

$$h^+_{VB} + H_2O \rightarrow H^+ + HO^{\cdot} \quad (9)$$

$$HO^{\cdot} + \text{Dye} \rightarrow \text{Intermediates} \quad (10)$$

$$O_2 + e^-_{CB} \rightarrow O_2^{\cdot -} \quad (11)$$

$$O_2^{\cdot -} + \text{Dye} \rightarrow \text{Intermediates} \quad (12)$$

$$O_2^{\cdot -},\ HO^{\cdot} + \text{Intermediates} \rightarrow CO_2 + H_2O \quad (13)$$

- Photogenerated hole (h^+) oxidation

$$h^+_{VB} + \text{Dye} \rightarrow \text{Decolorization/Intermediates} \quad (14)$$

RhB is a cationic florescent dye with at least three aromatic rings fused into a complex structure. It possesses a strong absorption band at λ_{max}=552 nm. The decolorization profile of RhB over 1 % W^{6+}-impregnated ZnO is presented in Fig. 1a, while the structural formula elaborating the complex binding and conjugation is presented at the onset of Fig. 1a. The percentage degradation of RhB over pure and W^{6+}-impregnated ZnO, evaluated from the UV-visible profiles, is

presented in Fig. 1b, where a significantly higher decolorization of dye can be observed for W^{6+}-loaded ZnO catalysts. In the initial 20 min of sunlight exposure, compared to ~7 % for bare ZnO, a decolorization of ~86, ~46, ~40, and ~14 % was observed for 1, 5, 10, and 15 % W^{6+}-loaded ZnO, respectively. The dye was completely decolorized (~100 %) by 1 % W^{6+}-loaded catalyst in 150 min of exposure. Compared to pure ZnO, a 10-fold increase in the decolorization was estimated for 1 % W^{6+}-impregnated catalyst. The graphical evaluation of the rate constants "k" for the decolorization of dye in the presence of pure and W^{6+}-impregnated ZnO catalysts obtained by applying Langmuir-Hinshelwood kinetics is presented in Fig. 1c, where a significantly higher rate of decolorization can be observed for impregnated catalysts. Compared to k= 0.0026 min^{-1} for pure ZnO, k=0.033 min^{-1} was observed for 1 % W^{6+}-impregnated ZnO. The observed high decolorization for impregnated catalysts compared to pure ZnO

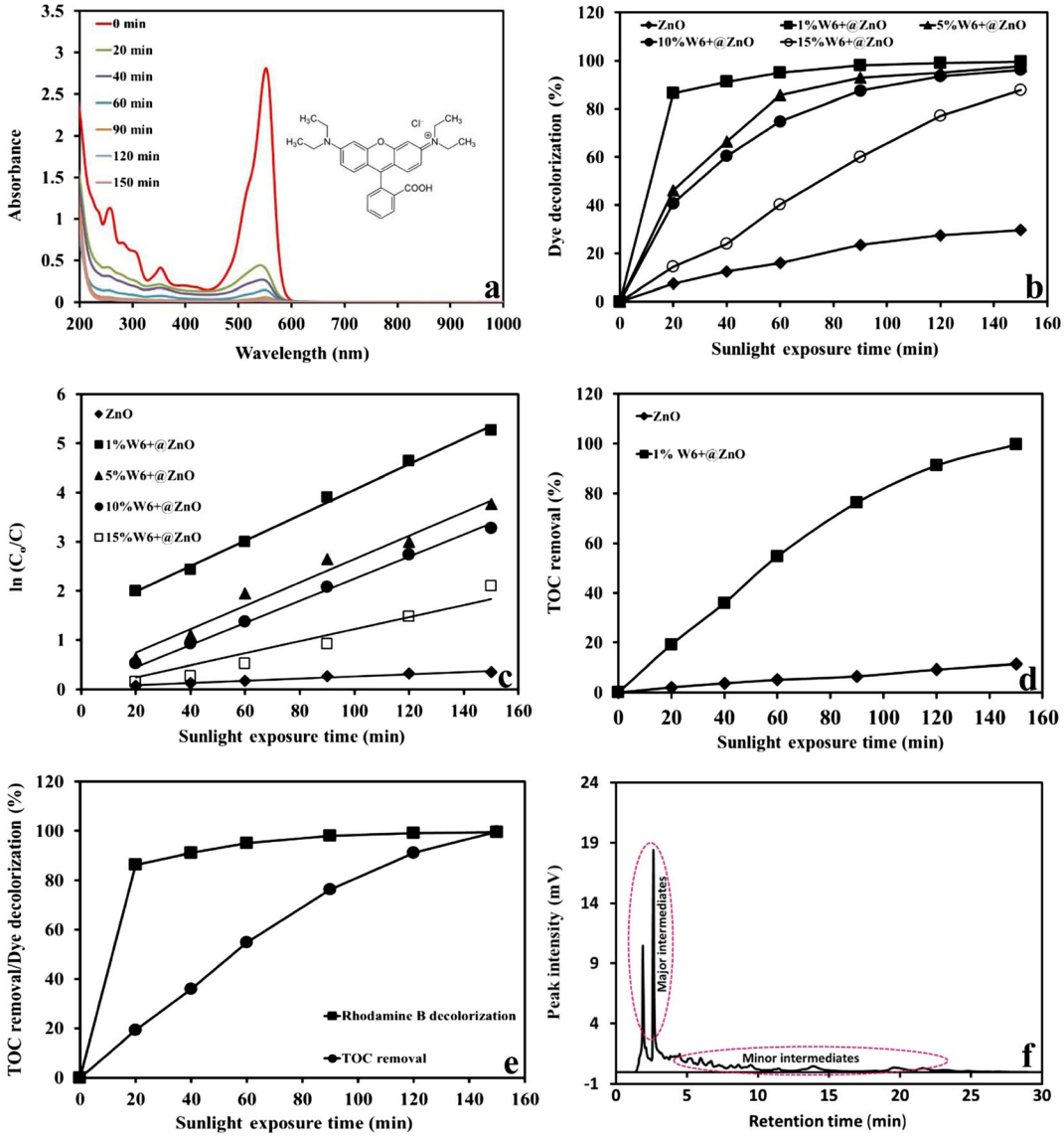

Fig. 1 **a** The UV-visible decolorization profile of rhodamine B over 1 % W^{6+}@ZnO. **b** The comparison of the percentage decolorization of RhB over pure and W^{6+}-impregnated ZnO. **c** The graphical evaluation of rate of decolorization. **d** The comparison of TOC removal over pure and 1 % W^{6+}@ZnO. **e** The comparison of decolorization and mineralization of RhB over 1 % W^{6+}@ZnO. **f** The HPLC profile of RhB over 1 % W^{6+}@ZnO after 20 min of sunlight exposure showing the intermediates formed

clearly indicates that the presence of W^{6+} at the surface of ZnO, a highly fluorescent material with high recombination rate, efficiently facilitates the "trapping" and "transfer" of photo-excited electrons. With favorable potential of the conduction band edge of ZnO (−0.31 V) for the reduction of O_2 to superoxide anion, the failure of pure ZnO in the efficient decolorization of dye depicts the loss of majority of charge carriers in recombination process. The significant decrease in the luminescence intensity in the PL spectra (Hameed et al. 2014) supports the trapping of excited electrons by surface W^{6+} species. The efficient decolorization especially by 1 % W^{6+}-loaded ZnO depicts the enhanced generation of oxidizing species in the system. It can be predicted that the oxygen surface-bonded W^{6+} states accept the photogenerated electrons from ZnO at the cost W^{6+}–O bond and form W^{5+} surface entities. The unstable W^{5+} states immediately transfer electrons to O_2 molecules in the vicinity and regain 6^+ oxidation states as elaborated below.

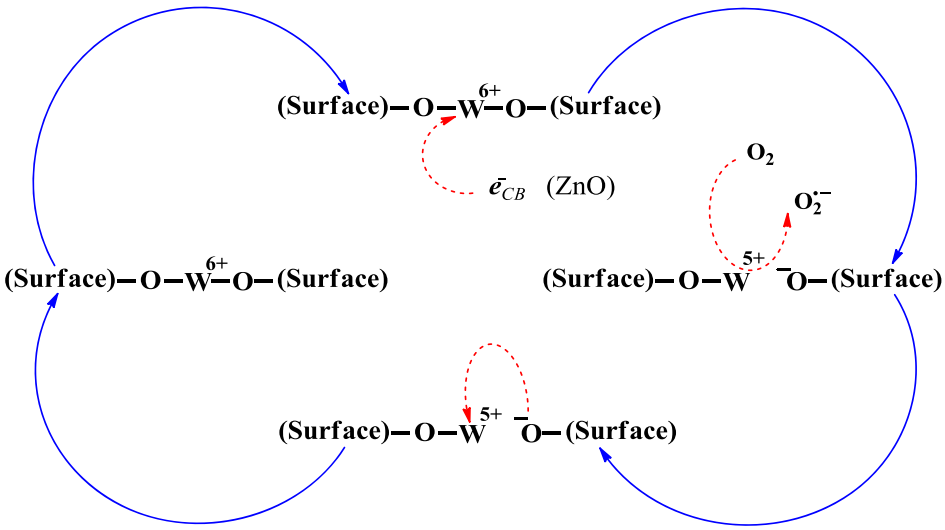

As mentioned earlier, the dyes lose their inherent color and absorption band with the loss of conjugation. Any minor change in the structure of dyes, i.e., interaction or insertion of any oxidizing specie in a photocatalytic system may result a decrease in the absorption intensity at a particular wavelength which is usually regarded as the degradation or mineralization. As per our view, the appropriate terminology that can practically explain this process is "decolorization." Therefore, the initial interaction of the oxidizing species (either $O_2^{\cdot-}$ or $HO^{\cdot}$ radicals) with the dye molecules leads to the decolorization of dye rather than degradation/mineralization, leaving behind a variety of intermediates. In dyes being high carbon-containing molecules, the true parameter that can differentiate between the mineralization and decolorization is the measurement of TOC. The comparison of TOC removal (%) as a function of time for bare and 1 % W^{6+}-impregnated ZnO is presented in Fig. 1d. A significantly higher mineralization, ~10 times, was observed for an impregnated catalyst. It is evident from Fig. 1e, showing the comparison of decolorization and mineralization for 1 % W^{6+}@ZnO, that the estimation of decrease in dye concentration by UV-visible spectroscopy is not the true measure of degradation/mineralization of the RhB. In comparison to ~80 % decolorization in the first 20 min of sunlight exposure, only ~20 % of TOC was eliminated in the same period. The disagreement between the two measurements suggests that initially, the oxidizing species interact with the giant dye molecules to split it into smaller intermediates, thus causing the fragmentation of dye with significant damages to the conjugated structure that results in the decolorization of dye. The rate of TOC removal increases with the decrease in dye

concentration, depicting the involvement of more and more oxidizing radical participates in TOC removal that were initially engaged in decolorization. ZnO has a favorable conduction band edge (−0.31 V) for the reduction of oxygen; therefore, the inevitable formation of superoxide anion radicals ($O_2^{\cdot-}$) can be predicted. The rapid decolorization of dye and removal of TOC indicated the pronounced role of $O_2^{\cdot-}$ in the oxidation process compared to any other oxidizing species such as $HO^{\cdot}$ radicals. The HPLC chromatogram of the RhB sample after 20 min of sunlight exposure confirmed the formation of intermediates (Fig. 1f). It is important to mention here that we failed to identify the substrate (RhB) in HPLC analysis under our experimental conditions detailed above but successfully separated the intermediates. The details discussed above lead to the conclusion that initially, the interaction of superoxide anion radicals ($O_2^{\cdot-}$) with dye molecules leads to decolorization with the formation of fragments. With the decrease in dye concentration with the increase in sunlight exposure time, the fragments are further oxidized by $O_2^{\cdot-}$ for complete mineralization. Probably, $HO^{\cdot}$ radicals due to their completely radical nature may not be able to decolorize and mineralize the dye so efficiently. Other researchers have also identified the leading role of superoxide anion radicals in photocatalytic processes as well (Turchi and Ollis 1990; Pichat 2013; Henderson 2011; Bielski et al. 1985). The fast decolorization rate also predicted that the direct photocatalysis (Eqs. 4–6) is the major mode of dye decolorization rather than indirect photocatalysis as the energy of photons absorbed by RhB (552 nm, 2.24 eV) may not be sufficient to induce charge separation (Eqs. 7–13). Keeping in view the charged as well as radical nature, the selectivity of $O_2^{\cdot-}$ for the particular interaction sites in the dye was evaluated by measuring the released anions in the solution during the course of experiment. Ion chromatography (IC) analysis identified NO_3^- ions in the solution which indicated the interaction of superoxide ions with terminal nitrogen-bearing groups. Being negatively charged in nature, $O_2^{\cdot-}$ anions seek fully or partially positive charge-bearing locations in the dye structure for interaction leading to decolorization. The insertion of the oxygen in the structure not only disturbs the conjugation but also imparts charge distortion due to the electronegativity. The successive interaction of oxygen leads to the formation of a variety of oxygenates with charge polarization, which further facilitates fragmentation and mineralization. The possible sites in RhB that can be interacted by $O_2^{\cdot-}$ anion radicals are identified in the Scheme 1.

AY is an "azo" dye with electron-withdrawing NO_2 group in the structure that imparts additional stability. The structure of AY is presented in the inset of Fig. 2a. AY is strongly absorbed in the 200–400-nm region of the spectrum, making a fraction of the photons inaccessible to the catalyst particles. The decolorization profile of AY over 1 % W^{6+}-impregnated ZnO catalyst in sunlight exposure is presented in Fig. 2a, while the comparison of timescale decolorization (%) of AY over bare and W^{6+}-impregnated ZnO is presented in Fig. 2b, where a significantly high decolorization of AY for all the impregnated catalysts compared to ZnO can be observed. Pure ZnO can utilize only 3–5 % of the solar spectrum, which comprises UV photons, for the generation of charge carriers (Rehman et al. 2009). The partial masking of the absorption region of ZnO by AY results in the significant decrease in the decolorization. The compatibility of the absorption regions of both ZnO and AY further strengthens the decolorization by indirect photocatalysis. AY molecules after being excited with the absorption of photons in 200–400 nm inject energy to the valance band of ZnO for band gap excitation. The resultant oxidizing radicals interact with the dye molecules, thus causing its decolorization. Although the dye molecules absorb the major portion of photons in 200–400 nm, the decolorization of dye molecules by direct photocatalysis cannot be ruled out. For bare ZnO, no decolorization of the dye was observed in the visible region of sunlight spectrum when the experiments were performed using a UV cutoff filter. Compared to ~38 % for bare ZnO, a decolorization of ~100, ~97, ~91, and ~78 % was observed for 1, 5, 10, and 15 % W^{6+}-impregnated ZnO in 150 min of sunlight exposure. The observed rate constants (k) evaluated for

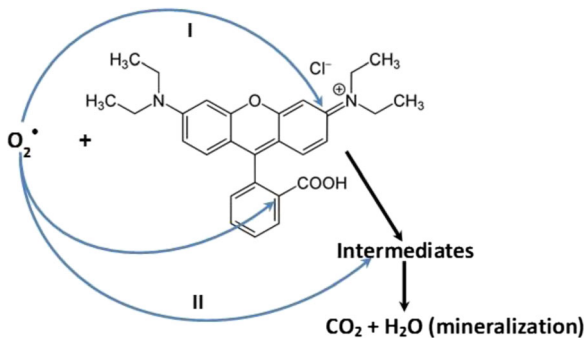

Scheme 1 Possible sites in RhB interacted by $O_2^{\cdot-}$ anion radicals

the degradation by plotting $\ln(C_o / C)$ versus sunlight exposure time, for pure, 1, 5, 10, and 15 % W^{6+}@ZnO were 0.0030, 0.036, 0.028, 0.018, and 0.012 min^{-1}, respectively. The comparison of TOC removal of bare and 1 % W^{6+}-impregnated ZnO revealed a significantly higher mineralization over 1 % W^{6+}-impregnated ZnO. Compared to <20 % TOC removal for pure ZnO, complete mineralization of AY was noticed in 150 min of sunlight exposure. The comparison of the AY decolorization and that of TOC removal (mineralization) is presented in Fig. 2c; ~97 % of the AY was decolorized in 90 min of sunlight exposure, while the same percentage of TOC was removed in 150 min, which again enlightens the initial engagement of superoxide ions and hydroxyl radicals with the complex AY molecules leading to fragmentation and decolorization. The HPLC profile (Fig. 2d) verified the fragmentation of AY. The intermediates further engaged in the oxidation process until complete mineralization. Based on the structure of AY, three positions can be identified that can be hospitable locations for $O_2^{\cdot-}$ anion attack. The presence of NO_2^- and COO^- auxochromes induces the partial positive charge on the attached carbon atom, making it a soft target for $O_2^{\cdot-}$ anions. In the presence of nitrite and nitrate anions in the solution, it can be assumed that the fragmentation of the dye structure is initiated with the displacement of terminal NO_2 groups by $O_2^{\cdot-}$ anions. The azo group (–N=N–), being part of the conjugated system, is another suitable location of the $O_2^{\cdot-}$ attack. The possible sites of interaction in AY are marked in Scheme 2.

MO, an azo dye with terminal SO_3^- group (inset of Fig. 3a), possesses a strong absorption band in the 200–550 nm range. The decolorization profile of MO on 1 % W^{6+}@ZnO catalyst is presented in Fig. 3a. As presented in Fig. 3b, all W^{6+}-impregnated ZnO catalysts showed superior activity compared to bare ZnO for the decolorization of MO. Compared to ~41 % for bare ZnO, ~100, 91, 67, and 50 % decolorization of MO was observed for 1, 5, 10, and 15 % W^{6+}-impregnated

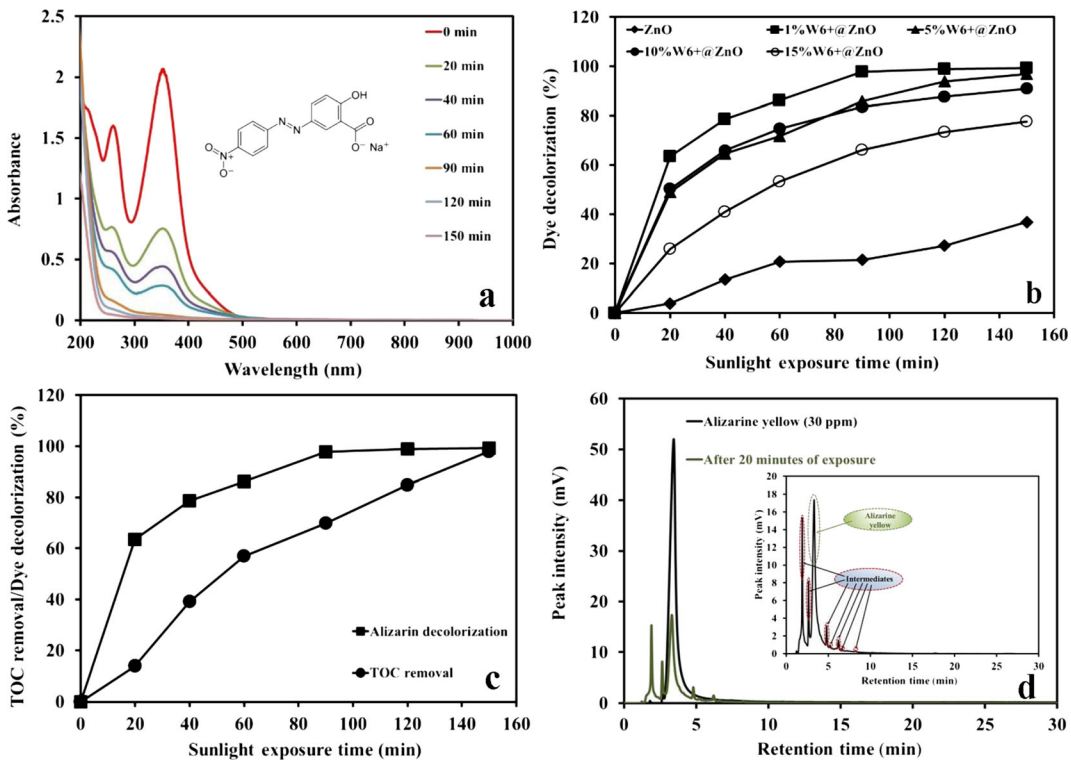

Fig. 2 **a** The UV-visible decolorization profile of alizarin yellow over 1 % W^{6+}@ZnO. **b** The comparison of the percentage decolorization of AY over pure and W^{6+}-impregnated ZnO. **c** The comparison of decolorization and mineralization of AY over 1 % W^{6+}@ZnO. **d** The HPLC profiles of AY (30 ppm) and after 20 min of sunlight exposure over 1 % W^{6+}@ZnO; the *inset* shows the intermediates formed

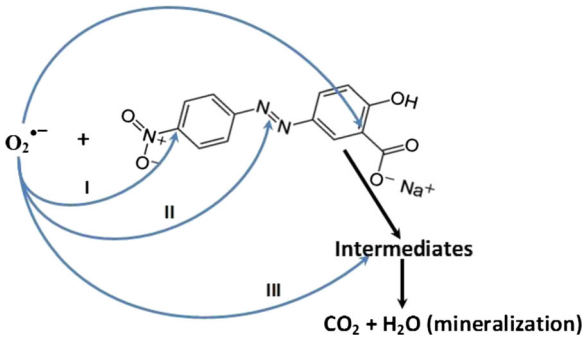

Scheme 2 Possible sites of interaction in AY

ZnO, respectively. The presence of strong absorption band in the excitation range of ZnO (200–400 nm) predicts that the decolorization of MO also proceed through indirect photocatalysis for bare and W^{6+}-impregnated ZnO photocatalysts. The low extent of decolorization for pure ZnO is due the nonavailability of efficient charge traps at the surface. The presence of W^{6+} states serves as boosters for enhancing the activity both by direct and indirect photocatalysis. The increasing surface density of W^{6+} states due to the loss of trapping and transfer ability of conduction band electrons imposes the detrimental effect on MO decolorization. The comparison of the MO decolorization and TOC removal efficiency of 1 % W^{6+}-impregnated ZnO is presented in Fig. 3c, where a substantial increase in the rate of depletion of TOC was observed with the decreasing concentration of MO. Figure 3d confirmed the possible formation of intermediates. The presence of SO_4^{2-} and NO_3^- ions in the solution confirms the displacement of terminal SO_3 groups by $O_2^{\cdot-}$ anion radicals as well as the interaction with the –N=N– group. The plausible locations in MO that can be targeted by $O_2^{\cdot-}$ anion radicals are (a) the carbon atom attached to NO_2 group, (b) the carbon atom attached to SO_3 group, and (c) the carbon atom attached to –N=N– group or the group itself after the loss of conjugation.

A rapid decolorization of CR was observed (Fig. 4a). CR is a di-azo dye with two terminal electron-withdrawing SO_3 groups (inset of Fig. 4a). It possesses a strong absorption band between 400 and 600 nm. A

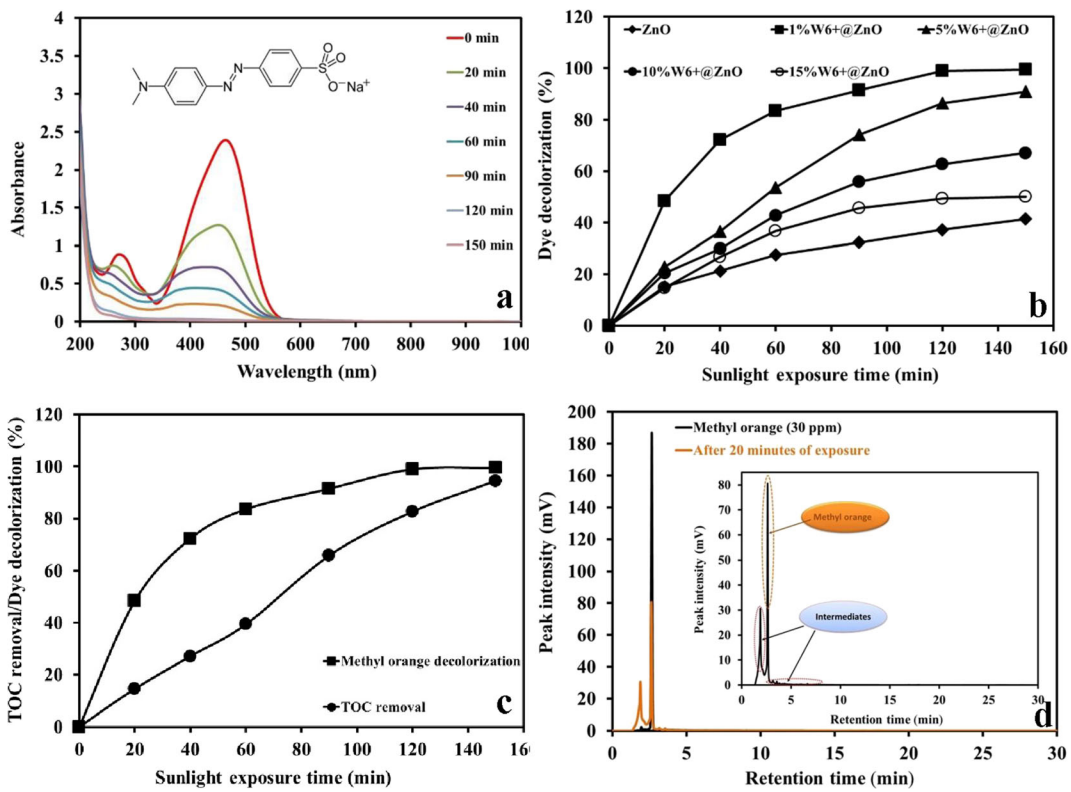

Fig. 3 **a** The UV-visible decolorization profile of methyl orange over 1 % W^{6+}@ZnO. **b** The comparison of the percentage decolorization of MO over pure and W^{6+}-impregnated ZnO. **c** The comparison of decolorization and mineralization of MO over 1 % W^{6+}@ZnO. **d** The HPLC profiles of MO (30 ppm) and after 20 min of sunlight exposure over 1 % W^{6+}@ZnO; the *inset* shows the intermediates formed

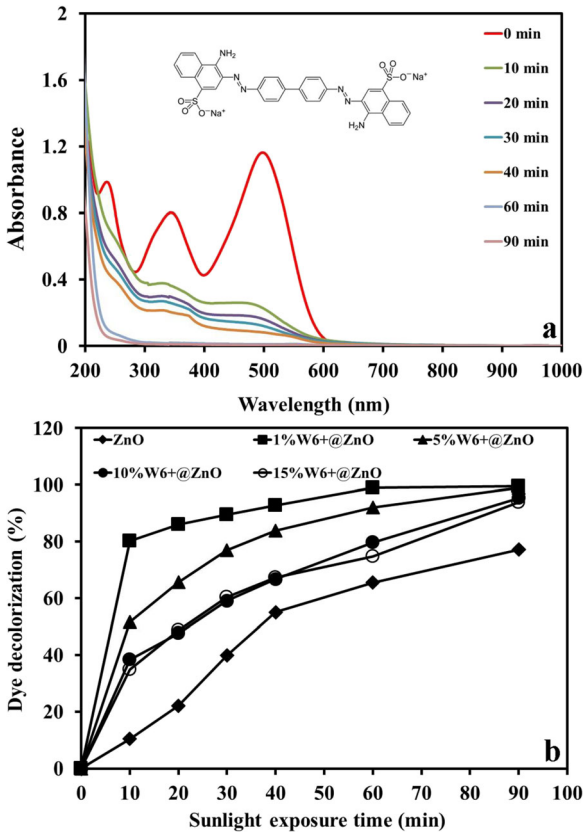

Fig. 4 **a** The UV-visible decolorization profile of congo red over 1 % W^{6+}@ZnO. **b** The comparison of the percentage decolorization of CR over pure and W^{6+}-impregnated ZnO

high decolorization of the dye was observed for all the catalysts, including ZnO. To establish the kinetics of decolorization although the experiments were performed for a period of 150 min, however, the samples were analyzed after every 10 min in the first hour instead of 20 min. The decolorization rate was found to be increasing with the decreasing concentration of dye in the solution. The timescale decolorization of CR is presented in Fig. 4b. Compared to ~77 % for bare ZnO, the decolorization of the dye on each W^{6+}-impregnated catalyst was higher than 90 % in 90 min of sunlight exposure. The rapid decolorization evidenced "direct photocatalysis" as the dominant mode. Complete decolorization of dye was accomplished in 90 min of sunlight exposure, while ~50 % mineralization was observed in the same period. A significant increase in TOC removal was observed with the decreasing CR concentration with time. The formation of intermediates in relatively higher concentration in HPLC analysis depicted the possible reason for low TOC removal compared to decolorization. The rapid decolorization of CR may be attributed to the terminal SO_3 and azo groups that serve as facilitators for the incoming $O_2^{\cdot-}$ anion radicals. The possible interaction sites in CR are (a) the carbon atoms attached to the terminal SO_3 groups and (b) the carbon atoms attached to the –N=N– groups.

IC, an anionic dye in nature, is a combination of fused (five- and six-membered rings) with two terminal SO_3 groups that do not possess a strong absorption band in 200–400 nm range (inset of Fig. 5a). It absorbs photons in the visible region at 610 nm. The degradation profile of IC is presented in Fig. 5a. A high decolorization of IC, as presented in Fig. 5b, was observed on all the catalysts, including ZnO in sunlight exposure. The decolorization of IC was even faster than that of CR. For 1 % W^{6+}-impregnated ZnO, ~90 % of the IC was removed in just 30 min; however, the same percentage of TOC was removed in 150 min. The carbon atoms

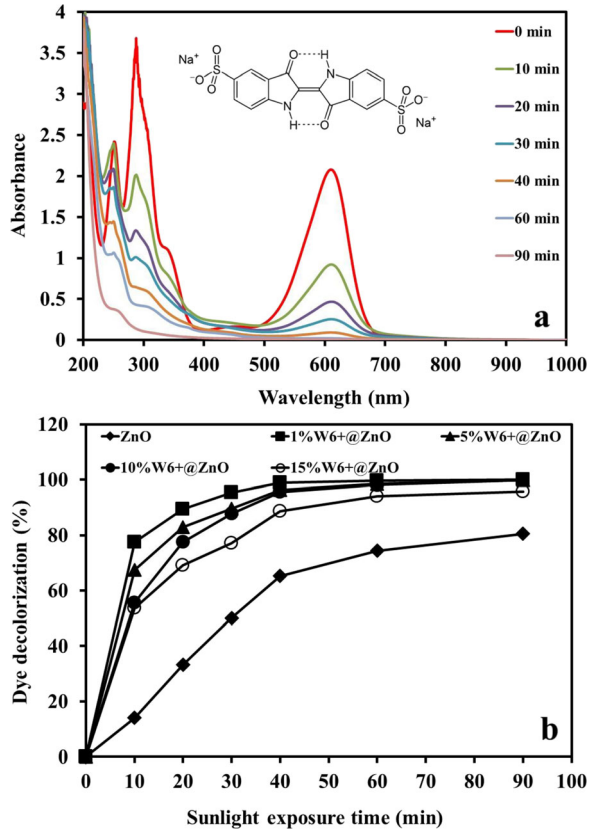

Fig. 5 **a** The UV-visible decolorization profile of indigo carmine over 1 % W^{6+}@ZnO. **b** The comparison of the percentage decolorization of IC over pure and W^{6+}-impregnated ZnO

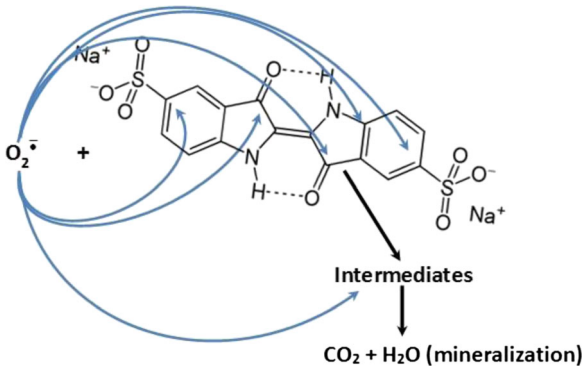

Scheme 3 Charge separation by intermolecular hydrogen bonding

attached to the electron-withdrawing SO_3 groups that are attached to the conjugated system are the soft interacting points for superoxide anions. Additionally, the charge separation induced by the intermolecular hydrogen bonding, as presented in Scheme 3, further facilitates the oxidation and mineralization of dye. An additional factor that accelerates the decolorization of the dye may be the interaction of the anionic IC with the photogenerated holes; however, no experimental evidence can be reported in this regard.

The structure of RB is presented in the inset of Fig. 6a. RB is a halogenated dye and has the absorption pattern similar to that of rhodamine B with absorption maximum at λ=547 nm. The decolorization profile of RB is presented in Fig. 6a. The rapid decolorization of RB was observed for all W^{6+}-impregnated catalysts including bare ZnO. As presented in Fig. 6b, for 1 % W^{6+}-impregnated ZnO, ≥80 % of the dye was decolorized in the first 10 min of sunlight exposure, while the complete decolorization was observed in 90 min of sunlight exposure. All the other catalysts including ZnO also decolorized ≥90 % of the dye in the same period. Although the dye was completely decolorized in 90 min, only ~80 % of the TOC was removed in the same period for 1 % W^{6+}-impregnated ZnO. The prolonged sunlight exposure removed ~96 % of TOC in 150 min; however, the rate of mineralization of RB was significantly higher than that of the other dyes. The rate of decolorization as well mineralization of RB is attributed to the higher number of sites available for $O_2^{\cdot-}$ anion radical interaction. The simultaneous interaction of $O_2^{\cdot-}$ at ~9–10 possible locations not only leads to the rapid decolorization of dye but also ends up with the formation of smaller fragments that are mineralized with ease leading to enhanced mineralization. The formation of fewer intermediates is also evidenced in Fig. 6c, the HPLC chromatogram recorded after 20 min of sunlight exposure. The rapid release of chloride and iodide ions, as measured by IC, was consistent with the timescale decolorization profile of the dye which confirmed the electron-withdrawing halogen groups (chloride and iodide) as the possible sites for $O_2^{\cdot-}$ anion radical attack to disrupt the conjugation-stabilized structures leading to the decolorization of the dye. The IC profile of the timescale release of Cl^- ions in the solution during photocatalytic process is presented in Fig. 6d. The appearance of ClO_4^- in the IC profile depicts that Cl^- is further interacted by the oxidizing species in the solution.

By the careful analysis of decolorization/mineralization data, it was observed that the number and the nature of the auxochromes attached to the conjugated system play a vital role in the decolorization process. The chemical nature of the substituent, whether electron withdrawing or electron donating, contributes in shifting the absorption spectra towards longer or shorter wavelength. The position and the number of electron-withdrawing groups facilitate the decolorization of dyes, while the release of these groups in the solution as respective anions with the progress of reaction clearly predicts the involvement of charged species in the process. The comparison of the decolorization (%) of RhB, AY, and MO is presented in Fig. 7a, while the inset shows the same for CR, IC, and RB. It can be noticed that although the structure of RhB is much complex, however, its decolorization was significantly higher than that of AY and MO. The possible reason may be the shifting of absorption maximum in the absorption region (200–400 nm) that hinders the direct absorption of photons by the catalyst particle, thus causing a decrease in the decolorization. The rapid decolorization of CR, IC, and RB is attributed to the electron-withdrawing nature and number of the auxochromes and other structural factors such as intermolecular hydrogen bonding and charge separation.

Superoxide $O_2^{\cdot-}$ anion radicals are the reactive charged entities that are instantly produced in the aqueous photocatalytic system. The factors that affect the population of these entities are already discussed in detail. The presence of additional charge in $O_2^{\cdot-}$ induces the instability and reactivity in these entities and requires

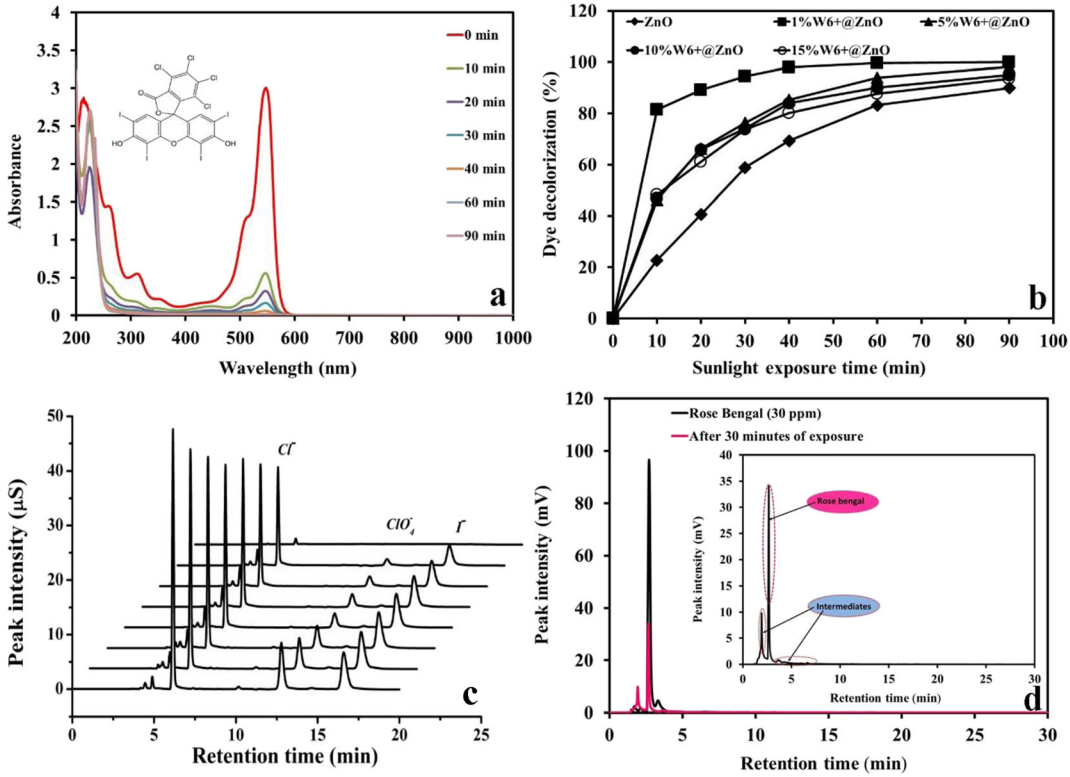

Fig. 6 **a** The UV-visible decolorization profile of rose bengal over 1 % W^{6+}@ZnO. **b** The comparison of the percentage decolorization of RB over pure and W^{6+}-impregnated ZnO. **c** the IC profile for the release of anions during the decolorization and mineralization of RB over 1 % W^{6+}@ZnO. **d** The HPLC profiles of RB (30 ppm) and after 20 min of sunlight exposure over 1 % W^{6+}@ZnO; the *inset* shows the intermediates formed

the instant dissipation of additional charge to regain stability (Pichat 2013). The presence of anions in the solution with the discharge of dye color depicts the involvement of charge entities like $O_2^{\cdot-}$ rather than hydroxyl radicals ($HO^{\cdot}$). Additionally, the rapid depletion of organic carbon supports the leading role of superoxide anion radicals; however, being among the primary oxidizers, the contribution of hydroxyl radicals in the decolorization process cannot be negated altogether.

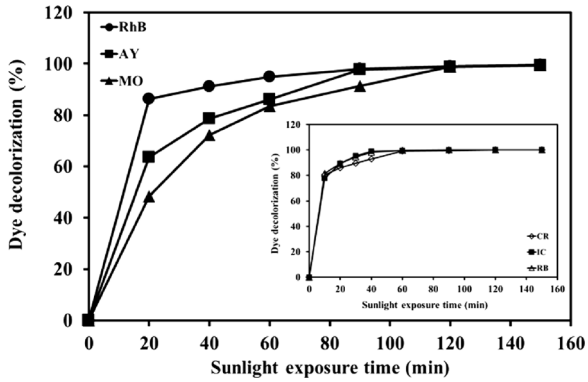

Fig. 7 **a** The comparison of the percentage decolorization of RhB, AY, and MO over 1 % W^{6+}@ZnO, while the *inset* shows the same for CR, IC, and RB. **b** The comparison of the percentage mineralization of RhB, AY, and MO over 1 % W^{6+}@ZnO, while the *inset* shows the same for CR, IC, and RB

The suitability of the most active among the synthesized catalysts, i.e., 1 % W^{6+}@ZnO, was evaluated for the decolorization and mineralization of the mixture of abovementioned dyes containing 10 ppm of each dye that doubled the overall dye concentration compared to individual dye. The decolorization profile of the mixture of dye is presented in Fig. 8. The decolorization of the mixture was evaluated on the basis of the peak at 550 nm. As presented in the inset of Fig. 8, the catalyst showed superior activity and ~96 % of the dye was decolorized in 150 min of sunlight exposure. The TOC removal was sluggish, and ~40 % mineralization was observed in the same period that is due to the increased

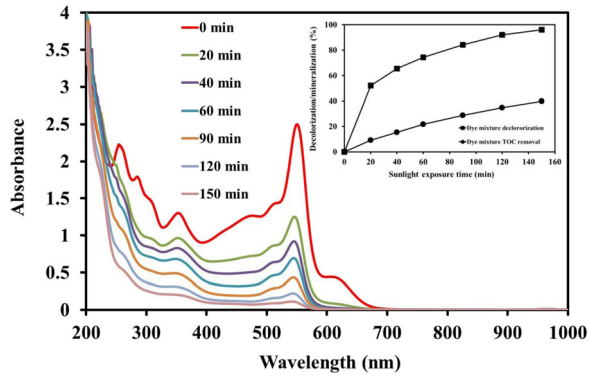

Fig. 8 **a** The UV-visible profile for the decolorization of the mixture of dyes (RhB, AY, MO, CR, IC, and RB) containing 10 ppm of each over 1 % W^{6+}@ZnO, while the *inset* shows the comparison of the percentage decolorization and mineralization of a mixture of dyes detailed above in sunlight exposure

dye concentration (almost twice as compared to individual dyes) and engagement of majority oxidation species in decolorization.

The consistency in the activity of 1 % W^{6+}-impregnated ZnO was evaluated by studying the degradation of RB with the same amount of catalyst three times in continuation by adding the fresh 30 ppm solution of the dye. The catalyst did not show any sign of deactivation, and a consistent performance was observed. As monitored by ICP, ≥1 ppm of Zn^{2+} ions in the solution was observed for W^{6+}-impregnated ZnO catalysts, which revealed the stability of the catalyst in the adopted experimental conditions.

Although the activity of all the W^{6+}-impregnated photocatalysts was much higher than that of bare ZnO, a successive decrease in the decolorization ability of the catalysts with increasing surface population of W^{6+} states was noticed. This observation led to the conclusion that the synergy, for the trap and transfer of photo-excited electrons, between ZnO and surface-bounded W^{6+} remains in operation up to a certain level of impregnation. Beyond this level, the mutual collaboration between the participating units is lost. The layer-by-layer deposition of W^{6+} ions at the surface with increasing impregnation leads to the decrease not only in the magnitude of effective charge trap and transfer. The low surface capacity of ZnO may be an additional contributor in this regard.

The above discussion can be summarized as follows:

- The loss of dye color during the photocatalytic process does not represent the removal of dye rather may be termed as decolorization.
- The TOC removal actually determines the removal of dye.
- The estimation of anions in the solution helps in identifying the oxidizing species involved.
- The superoxide anions displace electron-withdrawing groups, which leads to the loss of conjugation causing the decolorization of dye initially and simultaneously with the intermediates formed causing mineralization
- The nature and number of electron-withdrawing groups in the structure of dye facilitates the decolorization of dye.

4 Conclusions

The impregnation of ZnO by W^{6+} ions not only improved the absorption of light in the visible region of the solar spectrum but also successfully suppressed the unwanted e^{-}–h^{+} pair by promoting the delivery of photogenerated electrons to the reductants. It was observed that superoxide anion radicals lead to the photocatalytic decolorization and mineralization process. Being charged in nature, superoxide anions are selective

in attack and displace electron-withdrawing groups that lead to decolorization initially, simultaneously followed by mineralization. The ease of degradation of dyes depends on the nature and number of electron-withdrawing groups present in the dye structure. Both indirect and direct photocatalysis modes were observed in the dye removal process; however, the extant of indirect photocatalysis depends on the position of the absorption spectra of dye. The study proved that the existing catalysts could be made responsive in sunlight; however, the knowledge of the nature and chemical compatibility among the components is essential so as to lead the desired results.

Acknowledgments Iqbal M.I. Ismail, A. Hameed, and M. Aslam are thankful to the Center of Excellence in Environmental Studies, King Abdulaziz University (Project No. 2/W/1435), and the Ministry of Higher Education, Kingdom of Saudi Arabia, for support.

References

Abrahart, E. N. (1977). *Dyes and their intermediates* (pp. 1–12). New York: Chemical.

Ahmed, S., Rasul, M. G., Martens, W. N., Brown, R., & Hashib, M. A. (2010). Heterogeneous photocatalytic decolorization of phenols in wastewater: a review on current status and developments. *Desalination, 26*(1), 3–18.

Bell, A. T. (2003). The impact of nanoscience on heterogeneous catalysis. *Science, 299*, 1688–1691.

Bhatkhande, D. S., Pangarkar, V. G., & Beenackers, A. A. (2002). Photocatalytic degradation for environmental applications—a review. *Journal Chemical Technology Biotechnology, 77*, 102–116.

Bielski, B. H. J., Cabelli, D. E., & Arudi, R. L. (1985). Reactivity of $HO_2/O_2^{\cdot-}$ radicals in aqueous solution. *Journal of Physical and Chemical Reference Data, 14*(4), 1041–1100.

Boyter, H. A. (2007). Environmental legislations USA. In R. M. Christie (Ed.), *Environmental aspects of textile dyeing*. Cambridge: Woodhead.

Chatterjee, D., & Dasgupta, S. (2005). Visible light induced photocatalytic decolorization of organic pollutants. *Journal of Photochemistry and Photobiology C, 6*, 186–205.

Cho, I. H., & Zoh, K. D. (2007). Photocatalytic decolorization of azo dye (Reactive Red 120) in TiO_2/UV system: optimization and modeling using a response surface methodology (RSM) based on the central composite design. *Dyes and Pigments, 75*, 533–543.

Chong, M. N., Jin, B., Chow, C. W. K., & Saint, C. (2010). Recent developments in photocatalytic water treatment technology: a review. *Water Research, 44*, 2997–3027.

Christie, R. M. (2001). *Colour chemistry*. Cambridge: Royal Society of Chemistry.

ETAD (1997). German ban on use of certain azo compounds in some consumer goods. ETAD Information Notice No. 6, (Revised).

Fang, Y., Huang, Y., Liu, D., Huang, Y., Guo, W., & David, J. (2007). Photocatalytic decolorization of the dye sulforhodamine-B: a comparative study of different light sources. *Journal of Environmental Sciences, 19*, 97–102.

Fujishima, A., Rao, T. N., & Tryk, D. J. (2000). Titanium dioxide photocatalysis. *Journal of Photochemistry and Photobiology C, 1*, 1–21.

Fujishima, A., Zhang, X., & Tryk, D. A. (2008). TiO_2 photocatalysis and related surface phenomena. *Surface Science Reports, 63*(12), 515–582.

Hameed, A., Montini, T., Gombac, V., & Fornasiero, P. (2008). Surface phases and photocatalytic activity correlation of Bi_2O_3/Bi_2O_{4-x} nanocomposite. *Journal of American Chemical Society, 130*, 9658–9659.

Hameed, A., Montini, T., Gombac, V., & Fornasiero, P. (2009a). Photocatalytic decolourization of dyes on NiO-ZnO nanocomposites. *Photochemical and Photobiological Sciences, 8*, 677–682.

Hameed, A., Gombac, V., Montini, T., Graziani, M., & Fornasiero, P. (2009b). Synthesis, characterization and photocatalytic activity of NiO-Bi_2O_3 nano-composites. *Chemical Physics Letter, 472*, 212–216.

Hameed, A., Gombac, V., Montini, T., Felisari, L., & Fornasiero, P. (2009c). Photocatalytic activity of Zn modified Bi_2O_3. *Chemical Physics Letter, 483*, 254–361.

Hameed, B. H., Akpan, U. G., & Wee, K. P. (2011). Photocatalytic decolorization of acid red 1 dye using ZnO catalyst in the presence and absence of silver. *Desalination Water Treatment, 27*, 204–209.

Hameed, A., Aslam, M., Ismail, I. M. I., Chandrasekaran, S., Kadi, M. W., & Gondal, M. A. (2014). Sunlight assisted photocatalytic mineralization of nitrophenol isomers over W^{6+} impregnated ZnO. *Applied Catalysis B, 160–161*, 227–239.

Henderson, M. A. (2011). A surface science perspective on TiO_2 photocatalysis. *Surface Science Reports, 66*, 185–297.

Hernández-Alonso, M. D., Fresno, F., Suárez, S., & Coronado, J. M. (2009). Development of alternative photocatalysts to TiO_2: challenges and opportunities. *Energy and Environment Science, 2*, 1231–1257.

Jiuhui, Q. U. (2008). Research progress of novel adsorption processes in water purification: a review. *Journal of Environmental Sciences, 20*, 1–13.

Khataee, A. R., Vatanpur, V., & Amani Ghadim, A. R. (2009). Decolorization of C.I. Acid Blue 9 solution by UV/nano-TiO_2, Fenton, Fenton-like, electro-Fenton and electrocoagulation processes: a comparative study. *Journal of Hazardous Material, 161*, 1225–1233.

Lam, S., Sin, J., Abdullah, A. Z., & Mohamed, A. R. (2012). Decolorization of wastewaters containing organic dyes photocatalysed by zinc oxide: a review. *Desalination and Water Treatment, 41*, 131–169.

Lazar, M. A., Varghese, S., & Nair, S. S. (2012). Photocatalytic water treatment by titanium dioxide: recent updates. *Catalysts, 2*, 572–601.

Lettmann, C., Hinrichs, H., & Maier, W. F. (2001). Combinatorial discovery of new photocatalysts for water purification with visible light. *Angewandte Chemie International Edition, 40*, 3160–3164.

Ligrini, O., Oliveos, E., & Braun, A. (1993). Photochemical processes for water treatment. *Chemical Reviews, 93*, 671–698.

Makita, M., & Harata, A. (2008). Photocatalytic decolorization of rhodamine B dye as a model of dissolved organic compounds: influence of dissolved inorganic chloride salts in seawater of the Sea of Japan. *Chemical Engineering Processing, 47*(5), 859–863.

Martinez, C. A., & Brillas, E. (2009). Decontamination of wastewaters containing synthetic organic dyes by electrochemical methods. A general review. *Applied Catalysis B, 87*, 105–145.

Mills, A., Davies, R. H., & Worsley, D. (1993). Water-purification by semiconductor photocatalysis. *Chemical Society Reviews, 22*, 417–425.

Neppolian, B., Kanel, S. R., Choi, H. C., Shankar, M. V., & Murugesan, B. N. (2003). Photocatalytic decolorization of reactive yellow 17 dye in aqueous solution in the presence of TiO_2 with cement binder. *International Journal of Photoenergy, 5*, 45–49.

Pichat, P. (2013). *Photocatalysis and water purification: from fundamentals to recent applications* (1st ed.). Germany: Wiley-VCH.

Rauf, M. A., & Ashraf, S. S. (2009). Application of advanced oxidation processes (AOP) to dye decolorization—an overview. In A. R. Lang (Ed.), *Dyes and pigments: new research*. New York: Nova Science.

Rehman, S., Ullah, R., Butt, A. M., & Gohar, N. D. (2009). Strategies of making TiO_2 and ZnO visible light active. *Journal of Hazardous Material, 170*, 560–569.

Rolison, D. R. (2003). Catalytic nanoarchitectures-the importance of nothing and the unimportance of periodicity. *Science, 299*, 1698–1701.

Sakthivel, S., Neppolian, B., Shankar, M. V., Arabindoo, B., Palanichamy, M., & Murugesan, V. (2003). Solar photocatalytic decolorization of azo dye: comparison of photocatalytic efficiency of ZnO and TiO_2. *Solar Energy Materials and Solar Cells, 77*, 65–82.

Singh, K., & Arora, S. (2011). Removal of synthetic textile dyes from wastewaters: a critical review on present treatment technologies. *Critical Reviews in Environmental Science and Technology, 41*, 807–878.

Sotto, A., Lopez-Munoz, M. J., Arsuaga, J. M., Aguado, J., & Revilla, A. (2010). Membrane treatment applied to aqueous solutions containing atrazine photocatalytic oxidation products. *Desalination and Water Treatment, 21*, 175–180.

Sun, J. H., Dong, S. Y., Feng, J. L., Yin, X. J., & Zhao, X. C. (2011). Enhanced sunlight photocatalytic performance of Sn-doped ZnO for methylene blue decolorization. *Journal of Molecular Catalysis A: Chemical, 335*, 145–150.

Turchi, C. S., & Ollis, D. F. (1990). Photocatalytic degradation of organic water contaminants—mechanisms involving hydroxyl radical attack. *Journal of Catalysis, 122*, 178–192.

Velmurugan, R., & Swaminathan, M. (2011). An efficient nanostructured ZnO for dye sensitized decolorization of Reactive Red 120 dye under solar light. *Solar Energy Materials and Solar Cells, 95*, 942–950.

Zhang, J. Z. (1997). Ultrafast studies of electron dynamics in semiconductor and metal colloidal nano-particles: effects of size and surface. *Accounts of Chemical Research, 30*, 423–429.